Journal of the Korean Physical Society, Vol. 65, No. 11, December 2014, pp. 1820∼1824

Analysis of Line Broadening and Spectral Asymmetry in an All-fiber Torsional Acousto-optic Band-pass Filter

Ilhwan Kim and Kwang Jo Lee*
Department of Applied Physics, College of Applied Science, Kyung Hee University, Yongin 446-701, Korea

In-Kag Hwang
Department of Physics, Chonnam National University, Gwangju 500-757, Korea

(Received 18 August 2014, in final form 11 September 2014)

The transmission properties of an all-fiber torsional acousto-optic (AO) band-pass filter with a sub-nm bandwidth is studied. The device is based on torsional AO coupling in a highly birefringent (HB) optical fiber. The full width at half maximum (FWHM) measured in a conventional band (C-band) is 0.88 nm, which is compared with the theoretical value of 0.45 nm estimated by using the coupled mode theory. The line broadening and the spectral asymmetry observed in experiments are investigated in detail through our theoretical model and full numerical analyses. The influence of the non-uniformity in the birefringence of the HB fiber on the filter's transmission is analyzed quantitatively in terms of the change in the filtering bandwidth, the sidelobe asymmetry, and the resonance shift.

PACS numbers: 42.79.Jq, 42.81.Gs, 42.81.Qb, 42.81.Wg
Keywords: Fiber optics, Acousto-optic devices, Birefringence, Polarization controlling
DOI: 10.3938/jkps.65.1820

I. INTRODUCTION

Optical-fiber-based wavelength filters have played a critical role as essential components in communication and sensing systems to select an individual signal out of multiple wavelength channels transmitted simultaneously via a single optical fiber. Among the functionalities, important advantages of fiber-based filters include the low-loss combination of wavelengths and the support of routing, as well as the selection of a single channel or several channels out of a larger number of channels. One such device of interest is the all-fiber acousto-optic tunable filter (AOTF), which offers a number of superior features compared to other typical fiber-based implementations employing fiber Bragg gratings or long-period fiber gratings – *e.g.*, wide (~ 100 nm) and fast (< 100 μs) wavelength tunability and variable power transmission by using simple electric control [1, 2]. Flexural and torsional acoustic waves have both been exploited in various types of all-fiber AO devices, where the acoustic waves cause resonant coupling between two spatial modes in an optical fiber (for flexural waves) or two eigen-polarization modes in a highly birefringent (HB) fiber (for torsional waves) [1,2]. In particular, torsional AOTFs have attractive features relative to their flexural counterparts: simple reconfiguration between notch and band-pass operation types, polarization-independent operation, no spectral deterioration due to acoustic birefringence, low fluctuation in output power, and immunity to external perturbations such as fiber bending or physical contact [3,4]. Several shortcomings, such as a long interaction length and an intrinsic polarization dependence, have been solved, as reported in Refs. [3] and [4], and the techniques are based on coiling the HB fiber and employing a polarization diversity loop, respectively. We believe that our torsional AOTF scheme has no significant downside as compared to its flexural counterpart. Several types of HB fibers with form- or stress-induced birefringence have been employed for demonstrating torsional AOTFs, but in most cases, the measured bandwidths of the output spectra reached several nm [3]. In Ref. [4], a sub-nm bandwidth was reported in a torsional AOTF, but the result was obtained under a band-rejection-type operation. For specific applications, however, such as for separating one channel wavelength from unwanted spurious noise at different wavelengths in high-repetition-rate optical communication or high-resolution chemical sensing systems, developing a torsional AOTF with sub-nm bandwidth operating as a band-pass-type is highly desirable. The narrow bandwidth is expected to be readily achieved by employing a longer AO interaction length (L) of the fiber because the bandwidth is inversely proportional to L. In general, however, a longer

*E-mail: kjlee88@khu.ac.kr; Fax: +82-31-204-8122

fiber length increases the overall device size and, thus, can limit practical applications. In the flexural AOTFs, keeping the fiber straight under constant strain is important, otherwise, the spectral position of the resonance peak, as well as the shape of the output filter spectrum will be deteriorated significantly by both fiber bending and strain variation [5, 6]. Metal tube packaging has been used to protect the AO interaction region of the fiber to solve this issue, but it causes another resonance effect that decreases the AO mode coupling efficiency [7]. In contrast to the flexural counterpart, the immunity of the torsional AOTFs to physical perturbation allows a coil of long L, facilitating the realization of strain-free, reduced-size band-pass filters with sub-nm bandwidths [3,4].

In this paper, we demonstrate an all-fiber torsional AO band-pass filter with a sub-nm bandwidth. The narrow bandwidth is achieved by employing a 4-m-length single HB fiber strand that is much longer than the typical fiber length (∼ a few tens of cm) used for AO interaction in most previous demonstrations. The long fiber length is coiled with a 7-cm diameter in order to reduce the overall device size. The measured full width at half maximum (FWHM) is compared with the theoretical value estimated by using the coupled mode theory [8]. Because the filtering bandwidth is also affected by the dispersion properties of modal birefringence (*i.e.*, effective indices of two interacting polarization modes), as well as L, an cumulative non-uniformity in the birefringence along the long HB fiber can disrupt the resonance condition, resulting in a deterioration of the filter's transmission spectrum [9]. We investigate the line broadening, as well as the spectral asymmetry, observed in experiments in detail through our theoretical model and full numerical analyses. The influence of the non-uniformity in the birefringence of the HB fiber on the filter's transmission is analyzed quantitatively in terms of the change in the filtering bandwidth, the sidelobe asymmetry, and the resonance shift.

II. EXPERIMENTS AND ANALYSIS

Figure 1(a) shows a schematic design of the all-fiber torsional AOTF used for measurements, and its basic configuration is similar to that of the device reported in Ref. [4]. A torsional acoustic wave is generated by the acoustic transducer composed of a combination of two pieces of shear-mode lead-zirconate-titanate (PZT) plates vibrating 180° out of phase with each other. The PZT plates is attached to the bottom end facet of a cone-shaped glass horn with a hollow channel along its center axis, through which a HB fiber is inserted into the horn from the bottom to the tip so that the generated torsional wave can be effectively coupled to the fiber at the tip. The HB fiber used for experiment has an elliptical core with dimensions of 2×4 μm^2 to produce the form-

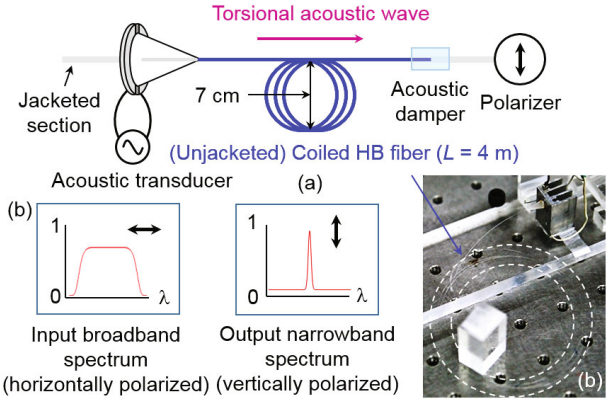

Fig. 1. (Color online) (a) Schematic design of the all-fiber torsional AO band-pass filter used for measurements. (b) Examples of input and output spectra of the filter. The arrows denote the polarization directions. (c) The main part of the device. The acoustic transducer with a glass horn is shown, and a 4-m-long bare fiber section of the HB fiber is coiled with a 7-cm diameter.

birefringence, and its outer diameter and modal birefringence (Δn_0) are 80 μm and 1.14×10^{-3} around 1550 nm, respectively. The 4 m-long bare fiber section for the AO interaction was coiled with a diameter of 7 cm, and an acoustic damper was placed at the end of the AO interaction region to remove travelling torsional acoustic waves. Macro-bending of the fiber, *i.e.*, fiber coiling of a few cm in radius as is in the case of our experiment, can induce additional birefringence to the fiber [10], which was calculated to be on the order of 10^{-8} under our experimental conditions. However, the result is one order of magnitude smaller than the minimum non-uniformity in the birefringence that can affect the filter spectrum, so that we concluded that the influence of coiling on the filter transmission was negligible, as will be discussed in Section III. Examples of the input and the output filter spectra are illustrated in Fig. 1(b). The input broadband light is polarized along one of the eigen-polarization axes of the HB fiber, which is coupled to the other eigen-mode while propagating through the AO interaction region by the applied torsional acoustic wave at the resonant wavelength satisfying the phase matching condition

$$\Lambda = L_B = \frac{\lambda}{\Delta n(\lambda)}, \tag{1}$$

where Δn, L_B, Λ, and λ denote the modal birefringence between two eigen-polarization modes, the polarization beat-length, and the acoustic and optical wavelengths, respectively. Λ is given by a tunable radio-frequency (RF) signal applied at the acoustic transducer, which determines the tunable resonant wavelength as shown in Eq. (1). The polarization axis of the output polarizer is set to be parallel to the polarization direction of the coupled light so that only the coupled light passes through the polarizer while the uncoupled light is rejected, leading to a band-pass operation. As shown in Fig. 1(c), the

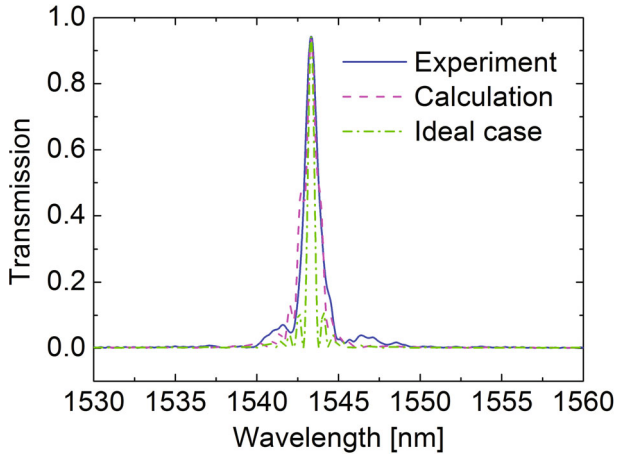

Fig. 2. (Color online) Transmission spectrum measured at the applied RF frequency of 2.748 MHz (solid line), ideal filter spectrum without axial non-uniformity in the modal birefringence (dash-dotted line), and calculated spectrum where the non-uniformity in the birefringence is considered to be $\Delta n_1 = 3.35 \times 10^{-7}$ and $\Delta n_2 = -0.5 \times 10^{-7}$, respectively (dashed line).

coiled fiber is laid on an optical table, allowing physical contact. In this case, the axial strain along the fiber is zero, no complicated packaging for strain management is required.

Figure 2 shows the transmission curves of the filter measured at an applied RF signal of 2.748 MHz (solid line) and calculated when the Δn non-uniformity was not present (dash-dotted line). The measured FWHM is 0.88 nm, which is the narrowest bandwidth among the previous demonstrations of all-fiber torsional AOTFs under band-pass operation. However, still the measured width is broader than the theoretical value of 0.45 nm estimated by using the coupled mode theory [5]. The asymmetric spectral shape with an increased bandwidth is interpreted as being due to the influence of the Δn non-uniformity on the filter's transmission [9]. The axial variation of n at a given wavelength can be expanded around the center of the AO interaction length (L) as follows:

$$\Delta n = \sum_{l=0}^{\infty} \Delta n_l \left(\frac{2}{L}\right)^l \left(Z - \frac{2}{L}\right)^l = \Delta n_0 + \frac{2\Delta n_1}{L}\left(Z - \frac{2}{L}\right) + \frac{4\Delta n_2}{L^2}\left(Z - \frac{2}{L}\right)^2 + \cdots, \quad (2)$$

where Δn_0 denotes the modal birefringence at resonance when the Δn non-uniformity does not exist. Δn_l represents the l-order amplitude of Δn profile defined as the maximum deviation of Δn_0 along L for each l. As can be expected from Eq. (1), a small increase (or decrease) of Δn along the fiber adds longer (or shorter) wavelength components to the filter's transmission as long as these components still satisfy the phase-matching condition. Note the even-order variation of the Δn profile (*e.g.*, for $l = 2$, the third term on the right side of Eq. (2)) has an even-function shape with respect to the center of L. This means that Δn increases (for positive values of Δn_2) or decreases (for negative values of Δn_2) partly on both sides of the center of L, resulting in enhancement of only either the right or the left wing of the transmission spectrum. Therefore, the spectral shape will become asymmetric. On the contrary, the odd-order variation of the Δn profile (*e.g.*, for $l = 1$, the second term on the right side of Eq. (2)) exhibits an odd-function shape with respect to the center of L; therefore, Δn increases on either side of the center of L but decreases on the other side. In this case, both longer and shorter wavelength regions from the center of resonance are enhanced simultaneously, resulting in a symmetric broadening of the resonance width with increased sidelobe levels.

As discussed above, the asymmetric spectral shape with a broadened transmission peak observed in Fig. 2 implies the existence of both even and odd orders of Δn_l. Here, we calculate only the linear (Δn_1) and the quadratic (Δn_2) amplitudes of the Δn profile because they exert a dominant influence on the transmission spectrum. Each value is estimated by fitting the transmission curve, where Δn_1 and Δn_2 are taken into account via the coupled mode theory [5]. The result shows that the estimated deviations are $\Delta n_1 = 3.35 \times 10^{-7}$ and $\Delta n_2 = -0.5 \times 10^{-7}$. The corresponding filter transmission curve including the calculated deviations (dashed line) is shown in Fig. 2, together with the measured filter spectrum (solid line). The curve indicates that a Δn non-uniformity of $\sim 10^{-7}$ that has accumulated along the 4 m of L causes a spectral broadening of resonance peak that is almost twice as much as the theoretical bandwidth of 0.45 nm.

III. DISCUSSION

Now using coupled mode theory as well as full numerical simulations, we investigate in more detail the influence of the Δn non-uniformity on the filter's transmission: namely, the influence of Δn_1 on resonance width and that of Δn_2 on the spectral asymmetry. In simulations, we keep the same parameters as were used in the experiment, *e.g.*, L, Δn_0, and the background noise level. The transmission curves calculated for several values of Δn_1 are plotted in Fig. 3(a). The results show that the overall filter spectra, as well as their resonance widths, become broader with increasing Δn_1 due to the spectral enhancement of both wings of the resonance peak, as described in the preceding section. The AO coupling efficiencies at the main peak(s) in each spectrum also decrease for larger Δn_1 at the same applied acoustic power because the power at the main resonance peak is exhausted by the AO coupling over the whole extended wavelength region. The FWHMs of the spectra are plot-

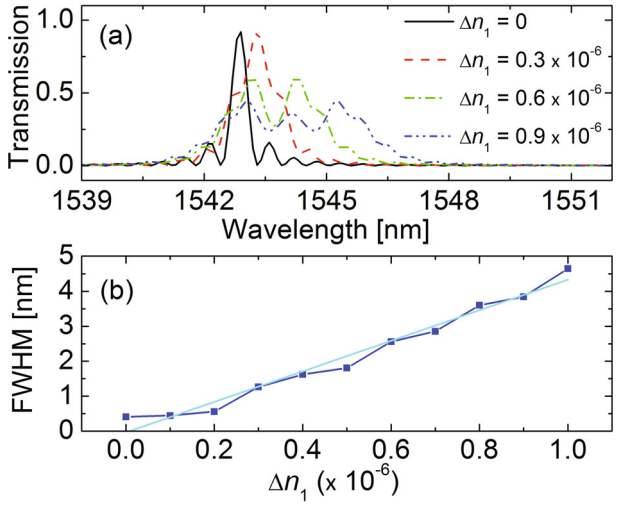

Fig. 3. (Color online) (a) Transmission curves calculated for increasing values of Δn_1, and (b) the corresponding FWHMs plotted as a function of Δn_1.

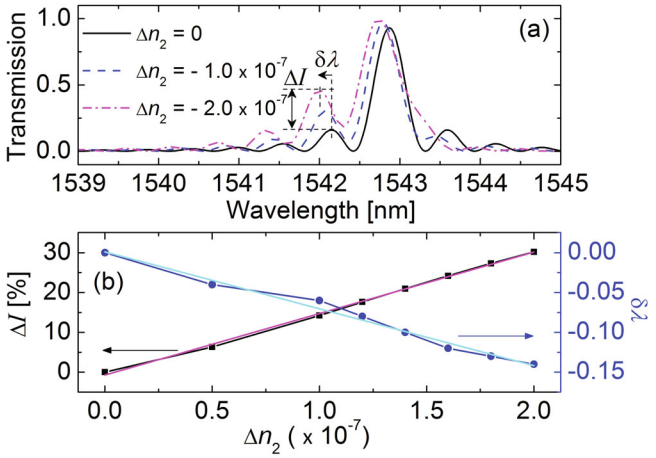

Fig. 4. (Color online) (a) Transmission curves calculated for increasing values of Δn_2, and (b) the enhancements of the second side peak (ΔI) and the spectral shift ($\delta\lambda$) plotted as functions of Δn_2.

ted in Fig. 3(b) as a function of Δn_1, showing an almost linear relationship with a slope of 4.37 nm per Δn_1 of 1.0 $\times$ 10^{-6}. Of course, a larger variation of Δn_1 will deteriorate the filter's spectrum significantly so that in that case, the FWHM does not follow a linear relationship with changing Δn_1.

The transmission curves calculated for several small values of Δn_2 are plotted in Fig. 4(a). As can be seen, the second side peak of the resonance increases with decreasing Δn_2, and its spectral position is blue-shifted as well. This is because a small decrease in Δn (negative values of Δn_2) along the fiber enhances the left spectral wing (the shorter wavelength region), as discussed earlier. Figure 4(b) shows the increase in the second side peak and the spectral shift plotted as functions of Δn_2. Here, ΔI and denote the difference in transmission at the second side peak and the shift of its spectral position when Δn_2 exists, as defined in Fig. 4(a). The result shows that both ΔI and $\delta\lambda$ exhibit almost linear relationships with respect to Δn_2 in the considered range. The estimated slopes of I and variations per Δn_2 of 1.0 $\times$ 10^{-7} are 15.44% and -0.07 nm, respectively. We note that for $|\Delta n_2| > 2.0 \times 10^{-7}$, the transmission curve starts to be deteriorated significantly by the increased sidelobe spectra. In this case, the side peaks are not well defined, and neither are ΔI and $\delta\lambda$.

IV. CONCLUSION

In conclusion, we have studied the influence of the non-uniformity in the birefringence on the transmission spectrum of the narrowband all-fiber torsional AO band-pass filter. The sub-nm bandwidth is achieved by employing a long AO interaction length of the HB fiber, and the measured bandwidth of the filter was 0.88 nm around a wavelength of 1550 nm for a HB fiber of 4 m in length. The measured filter spectrum exhibits an asymmetric shape with a broadened resonance peak, which was investigated through full numerical simulations in terms of line broadening, sidelobe asymmetry, and spectral shift. The results show that if sub-nm linewidth filtering is to be achieved, reducing the Δn non-uniformity to a level of $< 10^{-7}$ under the considered experimental conditions is critical, which means that the all-fiber torsional AO band-pass filter studied in this work has potential as an excellent tool for estimating the Δn non-uniformity of a HB fiber with a high accuracy of $\sim 10^{-7}$, which corresponds to a 0.1% variation in the value of Δn for typical HB fibers.

ACKNOWLEDGMENTS

This work was supported by a grant from Kyung Hee University in 2013 (KHU-20130396) and by the Basic Science Research Program through the National Research Foundation of Korea (NRF) funded by the Ministry of Science, ICT & Future Planning (NRF-2014R1A1A1002020).

REFERENCES

[1] H. S. Kim, S. H. Yun, I. K. Hwang and B. Y. Kim, Opt. Lett. **22**, 1476 (1997).
[2] M. Berwick, C. N. Pannell, P. St. J. Russell and D. A. Jackson, Electron. Lett. **27**, 713 (1991).
[3] K. J. Lee, I.-K. Hwang, H. C. Park and B. Y. Kim, IEEE Photon. Technol. Lett. **22**, 523 (2010).
[4] K. J. Lee, I.-K. Hwang, H. C. Park and B. Y. Kim, Opt. Express **17**, 6096 (2009).

[5] J. Zhao, X. Liu, Y. Wang and Y. Luo, Appl. Opt. **44**, 5101 (2005).
[6] A. Diez, G. Kakarantzas, T. A. Birks and P. St. J. Russell, Electron. Lett. **36**, 1187 (2000).
[7] S. H. Yun and H. S. Kim, IEEE Photon. Technol. Lett. **16**, 147 (2004).
[8] A. W. Snyder and J. Jove, Optical Waveguide Theory (Springer, New York, 1983).
[9] D. A. Smith, A. d'Alessandro, J. E. Baran and H. Hermann, Appl. Phys. Lett. **62**, 814 (1993).
[10] R. Ulrich, S. C. Rashleigh and W. Eickhoff, Opt. Lett. **5**, 273 (1980).